A peer-reviewed version of this preprint was published in PeerJ on 10 October 2019.

View the peer-reviewed version (peerj.com/articles/7703), which is the preferred citable publication unless you specifically need to cite this preprint.

Montagnani L, Badraghi A, Speak AF, Wellstein C, Borruso L, Zerbe S, Zanotelli D. 2019. Evidence for a non-linear carbon accumulation pattern along an Alpine glacier retreat chronosequence in Northern Italy. PeerJ 7:e7703 https://doi.org/10.7717/peerj.7703

Evidence for a non-linear carbon accumulation pattern along an Alpine glacier retreat chronosequence in Northern Italy.

Leonardo Montagnani[1,2*], Aysan Badraghi[1], Andrew F. Speak[1], Camilla Wellstein[1], Luigimaria Borruso[1], Stefan Zerbe[1] and Damiano Zanotelli[1].

[1] Faculty of Science and Technology, Free University of Bozen-Bolzano, Piazza Università 5, I-39100 Bolzano, Italy

[2] Forest Services, Autonomous Province of Bolzano, Via Brennero 6, I-39100 Bolzano, Italy.

Corresponding Author:
Leonardo Montagnani*
Piazza Università 1, Bolzano, Italy
Email address: leonardo.montagnani@unibz.it

Abstract

Background The glaciers in the Alps, as in other high mountain ranges and boreal zones, are generally retreating and leaving a wide surface of bare ground free from ice cover. This early stage soil is then colonized by microbes and vegetation in a process of primary succession. It is rarely experimentally examined whether this colonization process is linear or not at the ecosystem scale. Thus, to improve our understanding of the variables involved in the carbon accumulation in the different stages of primary succession, we conducted this research in three transects on the Matsch glacier forefield (Alps, N Italy) at an altitude between 2350 and 2800 m a.s.l.

Methods In three field campaigns (July, August and September 2014) a closed transparent chamber was used to quantify the net ecosystem exchange (NEE) between the natural vegetation and the atmosphere. On the five plots established in each of the three transects, shading nets were used to determine ecosystem response function to variable light conditions. Ecosystem respiration (Reco) and gross ecosystem exchange (GEE) was partitioned from NEE. Following the final flux measurements, biometric sampling was conducted to establish soil carbon (C) and nitrogen (N) content and the biomass components for each transect.

PeerJ Preprints | https://doi.org/10.7287/peerj.preprints.27703v1 | CC BY 4.0 Open Access | rec: 6 May 2019, publ: 6 May 2019

Results. A clear difference was found between the earlier and the later successional stage. The older successional stages in the lower altitudes acted as a stronger C sink, where NEE, GEE, and Reco were significantly higher than in the earlier successional stage. Of the two lower transects, the sink capacity of intermediate-succession plots exceeded that of the plots of older formation, in spite of the more developed soil. Total biomass (above- and belowground) approached its maximum value in the intermediate ecosystem. Whilst, the later stage of succession predominated in the corresponding belowground organic mass (biomass, N and C).

Outlook. We found that the process of carbon accumulation along a glacier retreat chronosequence is not linear, and after a quite rapid increase in carbon accumulation capacity in the first 150 years, in average 9 g C m^{-2} y^{-1}, it slows down, taking place mainly in the belowground biomass components. Concurrently, the photosynthetic capacity peaks in the intermediate stage of ecosystem development. If confirmed by further studies on a larger scale, this study would provide evidence for a predominant effect of plant physiology over soil physical characteristics in the green-up phase after glacier retreat, which has to be taken into account in the creation of scenarios related to climate change and future land use.

Introduction

Air temperature is increasing globally and glacier retreat is among the most striking evidence of global change (Walker & del Moral, 2003; Nakatsubo et al., 2005; Barry, 2006; Kozioł et al., 2014; Pepin et al., 2015), and this is particularly evident in the Alps. Due to increases of annual mean temperature, 75% of all Alpine glaciers are estimated to be retreating in the last 150 years, exposing the abundant bare substrate to plant colonization (Walker & del Moral, 2003). After the expansion peak occurred around 1860 (Solomina et al., 2016), the glaciers on the Alps, as in other mountain ranges and boreal zones, are generally retreating (Zemp et al., 2015; Sigl et al. 2018), leaving an abundance of bare ground free from ice cover. This emergent territory represents a new habitat for the biotic communities, i.e. bacteria, fungi, plants, and animals. The starting colonization by these taxa and their subsequent development can have direct effects on ecosystem functioning and element cycling.

The formation of the new biocenosis above former bare soil is defined as a process of primary succession (Odum, 1969; Walker & del Moral, 2011). In this process, microbes, vegetation, and

PeerJ Preprints | https://doi.org/10.7287/peerj.preprints.27703v1 | CC BY 4.0 Open Access | rec: 6 May 2019, publ: 6 May 2019

fauna are involved in the development of soil and in the accumulation of organic carbon (Matthews, 1992; Nakatsubo et al., 1998; Egli et al., 2001; Bekku et al., 2004; Nakatsubo et al., 2005; Burga et al., 2009; Yoshitake et al., 2011; D'Amico et al., 2014; Li et al., 2018). The soil, with its properties tied to its developmental stage, acts as a major player in the carbon accumulation process, with its increasing potential for carbon release as the carbon stock increases, but also with its increasing capacity for exchanging ions and sustaining the functions of photosynthetically active plants. Therefore, it represents a relevant variable when the formation of a new vegetation community is considered in a biogeochemical perspective.

The exposed terrain offers a mitigation potential for the global change, since the carbon sequestered by the newly established vegetation represents a negative feedback to the atmospheric increase of carbon dioxide and the consequent radiative forcing. This improvement in the long-wave energy balance component will partially offset the opposite effect in the short-wave energy balance due to reduced albedo after snow and glacier melting (Forzieri et al., 2017). Besides the global relevance of this phenomenon, it is scarcely defined which are the main variables involved in the process of vegetation regrowth. Different biological factors, including vegetation and microbe type, and the environmental constraints, in particular temperature, radiation and snow cover (Desai et al., 2016; Metcalfe et al., 2011) should be taken into account to explain the sink capacity along the different phases of vegetation regrowth. All of these variables interact with the chemical and physical properties of the soil and local microclimatic conditions and with the effect of human activity and released black carbon and nitrogen (Bradley et al., 2017).

An increasing number of studies have been undertaken in recently deglaciated terrain (Nakatsubo et al., 1998; Uchida et al., 2002; Bekku et al., 2004; Nakatsubo et al., 2005; Uchida et al., 2006; Yoshitake et al., 2007; Guelland et al., 2012; Chae et al., 2016). However, a gap in our current understanding exists around the linkage between current vegetation gas exchange and achieved level of soil evolution and overall carbon accumulation. Plants in the different phases of primary succession frequently also show different lifeforms: While the earliest stages are dominated by mosses and annual herbs (Raunkiaer Therophytes) at the final phase forbs with abundant underground lignified tissue (Hemi- and Cryptophytes) prevail. However, do these life forms and their functional traits have any influence on the velocity with which the carbon in the soil is accumulated?

PeerJ Preprints | https://doi.org/10.7287/peerj.preprints.27703v1 | CC BY 4.0 Open Access | rec: 6 May 2019, publ: 6 May 2019

We can hypothesize three different scenarios (Fig. 1). In scenario 0, both assimilation and respiration linearly increase along the chronosequence. In scenario 1, the physico-chemical characteristics of the soil and their positive feedback on assimilation capacity prevail, leading to a maximum sink capacity in the later stage of the chronosequence. In scenario 2, the effect of growth form and plant strategy prevails, leading to an assimilation and respiration pattern with a maximum sink at an intermediate stage.

The scenario 0 is used in the largely deployed biogeochemical models, like Biome-BGC (Running, & Gower, 1991; Thornton & Rosenbloom, 2005). In these models, a spin-up phase lasting hundreds of years is used to bring the ecosystem to stable conditions. In this scenario, the impact of vegetation type variation is not taken into account and the variation in carbon and nitrogen amounts is considered to influence equally photosynthesis and respiration.

In scenario 1, we hypothesize that soil evolution is more relevant for the fluxes than vegetation characteristics. Plant C and soil organic C are in active exchange with the atmosphere and small changes in soil organic C stocks could have severe impacts on the global C cycle (Knops et al., 2009; Wen-Jie et al., 2011; Cong et al., 2014; Walter et al., 2016; Luo et al., 2017). In addition, documented evidences revealed that the amount of nitrogen present in the soil and in the vegetation is strongly linked to ecosystem fluxes (Field & Mooney, 1983; Reich et al., 2006; Xia et al., 2009; Huff et al., 2015; Wang et al., 2015; Peng et al., 2017; Song et al., 2017; Tanga et al., 2018). Its evolution in time during the primary succession can be rightfully considered an independent variable influencing vegetation activity and biogenic fluxes.

In scenario 2, we hypothesize the prevalence of specific plant physiological traits over the soil developmental stage. The early stage of vegetation in the primary succession is known for the different biological strategy and functional traits, with higher assimilation rate but lower survival rate (Grime, 1977; Grime, 1988; Reich, 2014). Some researchers (e.g., Kimmins, 1987) suggest that at the beginning of each seral stage, net productivity will generally increase until perhaps the middle or later part of the stage, then level off, and finally decline somewhat as transition to the next stage occurs.

Given these contrasting drivers, in our studied ecosystem, we would like to know what are the relations between soil evolution, vegetation growth form, local climate and the observed patterns

PeerJ Preprints | https://doi.org/10.7287/peerj.preprints.27703v1 | CC BY 4.0 Open Access | rec: 6 May 2019, publ: 6 May 2019

of CO_2 exchange and carbon accumulation. We expect that the evolution in time of the soil and of the vegetation traits can act as intertwined variables in addition to climate.

Besides this overall question, the specific objectives of this research, which combined gas exchange with soil and vegetation carbon measurements along an alpine range in the Eastern Italian Alps, were the following:

1. Quantification of the organic carbon and nitrogen accumulated in the soil and in belowground (BG) and aboveground (AG) vegetation along a glacier retreat chronosequence.

2. Quantification of the net ecosystem exchanges (NEE), of the gross ecosystem exchange (GEE) and of the total ecosystem respiration (Reco) in the different stages of the chronosequence.

3. Assessment of the linkage between the degree of soil and vegetation evolution and the observed biological fluxes.

Understanding the variables involved in the process of carbon sequestration will help to model the vegetation regrowth after glacier retreat in similar alpine ecosystems, and also to build scenarios where the vegetation green-up after deglaciation is taken into account.

Material & methods

Study site

The study sites were in the upper catchment area of the Matsch valley, which is situated within a glacier retreated area in the north of Italy (Bozen/Bolzano in the Italian Alps, Fig. S1). Mean annual air temperature and precipitation (the mean values from the long-term observation 1970-2000), recorded at the closest weather station (Hydrographic Office of the Autonomous Province of Bozen-Bolzano) were 6.6 °C, and 550 mm at 1570 m a.s.l, where at 2000 m a.s.l precipitation increased up to 800-1000 mm (Penna et al., 2014). Further details about geomorphology and glacial cover are reported in Habler et al. (2009), Knoll et al. (2009) and Varolo et al. (2016).

Three study sites were set up in Val Mazia/Matschertal along three transects. The first transect (T1; early successional stage) was established at 2800 m a.s.l., next to the present-day glacier tongue (glacier 2800 m). The second transect (T2; intermediate successional stage) was established

PeerJ Preprints | https://doi.org/10.7287/peerj.preprints.27703v1 | CC BY 4.0 Open Access | rec: 6 May 2019, publ: 6 May 2019

at 2450 m a.s.l., but within the glacier extent of the 'Little Ice Age' (LIA), therefore covered by the ice until the year 1860 (Moraine LIA 2450 m). The last transect (T3; late successional stage) was conducted at 2350 m a.s.l., in an area that was outside the glacier tongue during the LIA which ended in the 19th century (Conoid 2350 m).

After a preliminary botanical survey, used to define the main plant species and communities present on the area, we used photographs taken on the collars to define the plant composition inside each collar. For plant identification, nomenclature and life form classification, we followed Zangheri (1976) and Dalla Fior (1981). For lichen identification and nomenclature, we followed the standard protocol of Smith et al. (2009) and Wirth et al. (2013), and for moss we followed Frey et al. (2006). Vascular plant species were assigned to taxonomic groups, i.e. monocotyledons and dicotyledons and to plant life forms (Raunkiaer 1934), i.e. Hemicryptophytes and Chamaephytes.

Gas exchange measurements

The experimental part of the research activity was carried out in three main distinct phases. After a preliminary survey in June, needed to identify transects to be sampled and to place the collars necessary to perform the gas exchange measurements, the first survey was done during the days 9th-11th of July. During these days, the first cycles of gas exchange measurements were conducted. The second cycle of measurements were conducted, with similar methods, in the period August 6-8; the third and last measurement cycle was performed in the period September 17-19.

The gas exchange measurements were done with the use of an automated closed transparent chamber (LI 8100-104C) attached to the analyzer LI 8100 (Li-Cor Biosciences, Lincoln, Nebraska, USA. The measurements (see Varolo et al, 2016; Galvagno et al., 2017; Pavelka et al., 2018; Zhao et al., 2018 for comparison and evaluation of the technique) were conducted on 15 numbered iron collars, 20 cm diameter, divided into groups of five plots (C1; …C5) in each of the three transects. To understand the response of the selected small ecosystem to solar radiation, Nylon filters having the same dimension of the collar were inserted in increasing number inside the chamber, in order to progressively intercept the solar radiation. Measurements were done in sequence, with an increasing number of filters (0, 1, 2, 3, 4, 5, 6, 7, 9, 11 and again zero filters). The final measurement, analog to the first in terms of radiation intensity (full light) was done to show a possible variation in the ecosystem response to light by reason of the temperature variation induced

PeerJ Preprints | https://doi.org/10.7287/peerj.preprints.27703v1 | CC BY 4.0 Open Access | rec: 6 May 2019, publ: 6 May 2019

by the presence of filters. Each measurement lasted 60 s, of which 20 s were considered as a dead band and 40 s used to assess the variation in time of the CO_2 dry mole density inside the chamber. Solar radiation, as expressed both in terms of energy and photon flux density, was assessed both inside and outside the filters by two distinct radiation sensors (Skye Instruments, Powis, UK). The combined use of sensors placed inside and outside the collar allowed the quantification of the reduction of light intensity caused by the progressive number of shading filters.

Soil and vegetation sampling and sample preparation

Following the final flux measurements, soil biometric sampling was carried out. The sampling was conducted on the entire AG vegetation and the soil below the collar up to 15 cm deep in the soil core. At each transect, five soil samples at three different depths, each one 5 cm deep (0-5, 5-10 and 10-15 cm) were sampled (n = 15 per transect and each depth interval), and total AG biomass was collected from each collar. A steel ring was used to collect the soil samples. Depending on stone characteristics, the ring was hammered inside the soil, and the stones placed around the ring were broken by using a lump hammer and a chisel or removed by a small shovel. Each sample was labeled and placed in a plastic bag for subsequent desiccation and laboratory analyses. The exact volume of the sample was determined by using plastic balls which were placed inside the collars. The plastic balls' volume was computed as a function of the balls' weight, which was measured at each sampling (ASTM, 1992).

In the laboratory, to compute soil moisture, all soil samples were weighed and then oven-dried at 105 ± 5°C until the sample reached a stable weight. Afterwards, the bulk density of the sampled soil was evaluated on the basis of measured volume and wet and dry soil density.

Sample analysis

The two portions of soil (fine soil and stones) and the roots were then brought to the laboratory, weighed and the dry fraction of soil and stones was determined. Sub-samples of stones and soil were placed separately in a mortar. Once pulverized, the material was analyzed. Roots were collected, weighed and analyzed separately.

The overall C content in the sampled volume was determined as the sum of the relative concentration of carbon, multiplied by the dry weight (DW) of roots, stones, and fine earth. The

PeerJ Preprints | https://doi.org/10.7287/peerj.preprints.27703v1 | CC BY 4.0 Open Access | rec: 6 May 2019, publ: 6 May 2019

soil was oven-dried and then weighed and acidified with Hydrochloric acid to eliminate the carbonate present (Brodie et al., 2011). The biomass and soil samples were analyzed for total carbon and nitrogen content and for the carbon isotopic ratio (δ^{13} C) by a FlashEA™ 1112 Elemental Analyzer (Thermo Fisher Scientific, Germany).

Statistical analysis

All statistical analyses were performed using R version 3.2.3 (R Development Core Team, 2013; www.r-project.org). The NEE value (µmol CO_2 $m^{-2}s^{-1}$) was obtained directly by the transparent chamber during the field measurement campaigns (July, August, and September), for each transect. The partitioning of NEE into GEE and Reco was assessed based on the well-established mathematical modelling approach of light response curves. This approach was modified to be suitable for measurements in small portions of the ecosystem, so as to include soil respiration. Afterwards, the values were used to obtain the mean daily dynamic course of NEE, GEE, and Reco (µmol m^2 s^{-1}). Analyses of residuals demonstrated that linear regression was frequently not appropriate for the determination of CO_2 fluxes by closed chamber methods, even if closure times were kept short (Kutzbach et al. 2007). We therefore used the recommended (Li-Cor, 2010) non-linear regression model

$$C'(t) = C'_x + (C'_0 - C'_x)e^{-\alpha(t-t_0)} \quad (1)$$

where $C'(t)$ is the instantaneous water-corrected chamber CO_2 mole fraction, C'_0 is the value of $C'(t)$ when the chamber closed and C'_x is a parameter that defines the asymptote, all in µmol CO_2 per mol dry air (µmol mol^{-1}); α is a parameter that defines the curvature of the fit (s^{-1}).

To fit carbon assimilation rates with light response curves, i.e., to verify the apparent response to light between PAR and measured NEE with transparent chamber in the three transects (T1, T2 and T3) in the months of July, August, and September 2014, we applied a logistic sigmoid model (Moffat et al., 2010; Eugster et al., 2010)

$$NEE = 2 \cdot F_{\infty} \left(0.5 - \frac{1}{1 + \exp\left(\frac{-2 \cdot \alpha \cdot PPFD}{F_{\infty}} \right)} \right) + R_d \quad (2)$$

PeerJ Preprints | https://doi.org/10.7287/peerj.preprints.27703v1 | CC BY 4.0 Open Access | rec: 6 May 2019, publ: 6 May 2019

where PPFD (photosynthetic photon flux density) is the driving variable, and α (initial quantum yield, alfa), F_{∞} (maximum NEE at full light) and R_d (daytime ecosystem respiration) are the three model parameters.

NEE and GEE at the PPFD of 2000 µmol m^{-2} s^{-1} (NEE2000, GEE2000) were calculated based on Eq.1. A detailed description of this calculation can be found in Schmitt et al. (2010). The ecosystem respiration at a reference temperature of 10°C (R10) was assessed using an Arrhenius type model (Lloyd and Taylor, 1994)

$$\mathrm{Re}co = R_{ref} \cdot e\left[E_0 (0.0178507 - \frac{1}{T + 46.02}\right] \qquad (3)$$

where R_{ref} is the respiration flux at the constant reference temperature T_0=10°C, E_0 is an empirical parameter which indicates the temperature sensitivity of Reco, and T is the air temperature in ˚C.

The flux differences between transects in each measurement campaign were determined by conducting a one-way ANOVA (Tukey b, $p < 0.05$). Further, to examine the effect of transects on the accumulated C and N in the soil, roots and AG vegetation, a one-way ANOVA (Tukey b, $p < 0.05$) was used.

The linkage between NEE, GEE and Reco and environmental variables (such as AG biomass (dry weight), nitrogen content in AG vegetation, carbon content in AG vegetation, BG biomass (dry weight), nitrogen content in BG vegetation, carbon content in below-vegetation, soil nitrogen, soil carbon) was tested by multiple linear regression.

Results

Plant species and vegetation

We have characterized a total of 19 species within collars (Table 1). According to our identification, the T1 study site, incompletely covered by vegetation, was characterized by one moss and one vascular plant species (*Pohlia filum* and *Poa laxa*, none of which was present in the other transects. T2 and T3 sites were fully covered by vegetation. T2 was characterized by 13 species, six of which were in common with T3. Four additional species at that site made a total of 10 species there. In T2, the most common species were *Festuca halleri*, *Lotus alpinus* and the moss

PeerJ Preprints | https://doi.org/10.7287/peerj.preprints.27703v1 | CC BY 4.0 Open Access | rec: 6 May 2019, publ: 6 May 2019

Racomitrium canescens, while in T3 the most common species were *Loiseleuria procumbens* and *Potentilla erecta.* Accordingly, the vegetation could be characterized as an alpine scree community of the Androsacion alpinae alliance (T1), as initial stages of alpine grassland of the Caricion curvulae alliance (T2) and as wind-exposed ridges Loiseleurio-Vaccinion alliance (T3) (e.g. Leuschner & Ellenberg, 2017). Full details on species composition in each collar are given in Table 1

Flux parameters patterns

The mean flux parameters (± SD, NEE, GEE, and Reco) that were measured during the field campaigns (July, August, and September 2014) in the different stages of the chronosequence are presented in Fig. 2. Negative flux represents CO_2 uptake and a positive one the reverse. The mean daily NEE was -1.2 ± 0.9 (mean ± SD), -7.6 ± 0.6 and -6.3 ± 0.4 g C m^2 d^{-1}; the mean daily GEE was -2.1 ± 1.3, -11.7 ± 0.6, -10.4 ± 1.1 g C m^2 d^{-1}; and the mean daily Reco was 0.8 ± 0.6, 4.1 ± 1.1, 4.1 ± 1.0 g C m^2 d^{-1} across the transects (Figure 2). Figure 2 shows that the daily mean value of NEE, GEE, and Reco in the earlier stage of succession is lower than T2 and T3, significantly.

During the vegetation seasons, in the different stages of the chronosequence, NEE response to PPFD in T2 and T3 showed similar trends and increased with increasing PPFD, whilst, this response was almost negligible (particularly in July) in the earlier stages of succession (Figure 3). Figure 3 shows that the light response curve line for NEE in T2 was located lower than T3 Additionally, the maximal negative value of NEE in T3 (July = -6.5, August = -6.5, and September = -5.9 µmol $m^{-2}s^{-1}$) was lower than T2 (July = -7.4, August = -6.9, and September = -8.0 µmol $m^{-2}s^{-1}$), which demonstrates the greater CO_2 sink capacity in T2.

For comparison across the chronosequence, we mainly followed the indication of Schmitt et al. (2010), and we used NEE2000, GEE2000 and the ecosystem respiration at a reference temperature of 10 °C (R10). The mean NEE, GEE, and alfa as measured during the field campaigns were the highest for the LIA moraine, significantly, and the lowest for the glacier (Figure 4). Across the chronosequence, the highest mean value of Reco was recorded for LIA moraine during July. Conversely during August and September, it was highest in conoid (Figure 4). Reco reached the highest mean value in August (T1 = 1.6 ± 0.9, T2 = 4.9 ± 1.7, and T3 = 5.5 ± 1.4 µmol $m^{-2}s^{-1}$), which was the warmer period during the study (T1 = 13.6 ± 1.3, T2 = 13.0 ± 1.7, and T3 = 16.8 ±

PeerJ Preprints | https://doi.org/10.7287/peerj.preprints.27703v1 | CC BY 4.0 Open Access | rec: 6 May 2019, publ: 6 May 2019

2.4˚ C), whereas the lowest value was observed in September, a period with the lowest air temperature during the study (T1 = 6.2 ± 1.5, T2 = 9.9 ± 1.8, and T3 = 10.4 ± 1.2 ° C).

For all the three transects, the highest mean value of NEE was observed in September (T1 = -5.9 ± 4.3, T2 = -11.3 ± 6.6, and T3 = -8.0 ± 8.3 µmol $m^{-2}s^{-1}$ and the most negative value recorded in August for T2 and T3 (T2= -8.5 ± 4.4, T3 = -6.4 ± 0.7 µmol $m^{-2}s^{-1}$) and July for T1 (-1.9 ± 3.8 µmol $m^{-2}s^{-1}$). September and July showed a much higher value of NEE for T2 and T3 (Figure 4). The highest mean GEE value was -6.6 ± 4.2, -15.6 ± 5.0, and -12±3.0 µmol $m^{-2}s^{-1}$ in T1, T2, T3, respectively. The greatest amplitude of GEE occurred in July for T2 and T3, and in September for T1.

Organic carbon and nitrogen content

We calculated the mean (±SD) accumulated C and N content in the soil, roots, and AG biomass in the three transects (Figure 4 and Table 2). The amount of C and N concentration in the soil was 40 ± 12 g C m^{-2} and 22 ± 3.4 g N m^{-2} near the glacier, 557 ± 115 g C m^{-2} and 58 ± 10 g N m^{-2} in the LIA moraine and 384 ± 98 g C m^{-2} and 59 ± 8.9 g N m^{-2} in the conoid, respectively. AG biomass, C and N mass increased across the chronosequence but was not significantly different between transects (Table 2). Moreover, C and N mass and AG biomass in the LIA moraine were higher than glacier and conoid ($P > 0.05$, Table 2).

The accumulated biomass, C and N mass in the BG vegetation (roots and rhizomes) increased significantly during the ecosystem development. Observed biomass, C and N mass in the BG vegetation was 58 ± 78, 1774 ± 385, and 2062 ± 411g m^{-2}; and 24 ± 34, 753 ± 157, and 959 ± 183 g C m^{-2} 0.36 ± 0.5, 20.0 ± 5.4, and 2.4 ± 6.3 g N m^{-2} in the three transects (Table 2). The biomass and C mass of BG vegetation were higher at T3 than at T1 and T2, significantly (Figure 5, Table 1), whilst N in BG vegetation was significantly higher at LIA moraine than glacier and conoid (Figure 5, Table 2).

The majority of C, N, and biomass were accumulated in BG vegetation while C, N and biomass accumulation aboveground were lower (Figure 5c, 3d, 3e, 3f, 3g, 3h). In T1 and T2, no significant differences can be seen between AG and BG C, N, and biomass but in T3 accumulated C, N, and

PeerJ Preprints | https://doi.org/10.7287/peerj.preprints.27703v1 | CC BY 4.0 Open Access | rec: 6 May 2019, publ: 6 May 2019

biomass in roots were significantly higher than AG vegetation (biomass p = 0.001, carbon p = 0.002, nitrogen p = 0.01).

Soil profile analyses

C and N content increased across the chronosequence in the soil profile significantly ($p < 0.001$). The highest values of C and N content were found in the conoid 2350 m (C = 7770 and N = 443 g m^{-2}) and the lowest value was found in the glacier 2800 m (C = 861 and N = 96 g m^{-2}, Figure 6). The majority of C and N accumulation were observed in the first level of soil profile near the soil surface, in the top 5 cm of the soil profile (T1 = 70.0%, T2 = 44.6%, T3 = 61.3% for C; and T1 = 54.6%, T2 = 44.5% and T3 = 55.0% for N). Soil C and N mass in this depth (~-2.5 cm) of the soil profile was significantly greater than at other soil depths (~-7.5,~ -12.5, $p < 0.001$). With increasing soil depth, C and N mass in the soil profile decreased significantly (Figure 6, $p < 0.001$).

At ~2.5 cm above the soil profile, the total C and N contents were significantly different ($p < 0.001$). The highest amount of C and N were found in the LIA moraine 2550 m (C = 1177 g C m^{-2} and N = 38 g N m^{-2}) and the lowest amount was found in the glacier 2800 m (C = 114 g C m^{-2} and N = 2.63 g N m^{-2}, Figure 6).

Soil bulk density decreased along the glacier retreat chronosequence. The highest value of bulk density was found in the glacier 2800 m (1.76 kg dm^{-3}) and the lowest value was found in the LIA moraine 2550 m (1.41 kg dm^{-3}). Soil bulk density increased with increasing soil depth significantly (T1 $p = 0.02$, T2 $p < 0.001$, T3 $p < 0.001$). The lowest value was found near the soil surface at the ~-2.5 cm depth of soil profile (T1 = 1.42, T2 = 0.66 and T3 = 0.63 kg dm^{-3}), while the highest value was at a depth of about -12.5 cm (T1 = 1.99, T2 = 1.84 and T3 = 1.94 kg dm^{-3}, Figure 6c). In the top level of the soil profile (~-2.5 cm), the bulk density was significantly changed across the chronosequence ($p = 0.007$) but this change was not significant in level 2 (~-7.5 cm, $p = 0.27$) and level 3 of the soil profile (~12.5 cm, $p = 0.44$).

Finally, we provide an assessment of the net production (µmol $m^{-2}s^{-1}$) and mean accumulated C (total AG, BG and soil C, kg m^{-2}) along the chronosequence of the primary succession after glacier retreat. As shown in Figure 7, the highest net production and total C was observed in T2 and the lowest in T1. This worthy and peculiar finding is indicating that the net production and total C

PeerJ Preprints | https://doi.org/10.7287/peerj.preprints.27703v1 | CC BY 4.0 Open Access | rec: 6 May 2019, publ: 6 May 2019

(AG, BG, and soil) approached their maximum value in the middle ecosystem (T2) instead of the older ecosystem (T3).

Assessment of the linkage between soil and vegetation evolution and the observed biological fluxes

The linkage between NEE, GEE, and Reco and site variables (AG and BG biomass, C and N, soil C and N, air temperature) was tested by multiple linear regression. Preliminary backward deletion procedure, following the Akaike information criterion (AIC), was applied to identify the most relevant variables influencing the biological fluxes. Then, the relaimpo R package was used to build modelling equations. We found that, over the whole season, the flux better explained by site conditions was Reco (80.57% variance explained by five regressors: C AG, DW BG, C BG, Nsoil, and Tair,), while GEE and NEE variability was explained to a lower extent (54.82% and 41.19 respectively) by a reduced set of variables (DW BG and C soil in both cases, and Tair only for NEE, see Table 3).

Discussion

Flux parameter pattern

Our results indicate that the LIA moraine and conoid, as intermediate and older successional stages, acted as a larger C sink, with NEE, GEE, alfa and Reco significantly higher than glacier foreground (earlier successional stage). This finding is in line with those of Nakatsubo et al. (1998; 2005), Bekku et al. (2004), Guelland et al. (2012), and D'Amico et al. (2014), who found the higher flux parameters in the later stages of succession.

All the flux parameters related to assimilation, namely NEE, GEE, and alfa, approached their highest value in T2 during all three field campaigns, although for some values the difference with T3 was not significant (Figure 2). Meanwhile, the highest mean value for Reco was recorded in T3 during August and September (Figure 4, $p > 0.05$) The higher flux parameters, and particularly the quantum yield of assimilation (alfa) in T2, are consistent with the well-established positive relationship between species richness and productivity (e.g., Waide et al., 1999).

PeerJ Preprints | https://doi.org/10.7287/peerj.preprints.27703v1 | CC BY 4.0 Open Access | rec: 6 May 2019, publ: 6 May 2019

The observed higher Reco in T3 can be explained by the higher BG biomass, C and N content (Tables 2 and Figure 5), which may result in a higher autotrophic respiration (Bekku, 2004; Guelland et al., 2012). On the other hand, it is well known that temperature has a strong effect on soil and plant respiration, and generally, the soil respiration rate would increase under future global warming (Oechel & Vourlitis 1994; Bekku et al. 2004; Eugster et al., 2010). In all three transects, Reco reached the highest mean value in August and lowest in September, respectively the warmest and coldest periods during the study. Apparently, the greater Reco led to a lower NEE. In fact, NEE reached the highest value in the coldest period (September) and the lowest value in the warmest period (August).

Organic carbon and nitrogen content

We quantified the organic C and N accumulated in soil, BG, and AG vegetation in the different stages of the primary succession, as one of our objectives (Figure 5 and Table 2). We found an increase of organic C and N accumulation in soil, BG and AG vegetation with ecosystem development, as has been recorded by several researchers in recently deglaciated terrain in the Alps (Matthews, 1993; Egli et al., 2001; Burga et al., 2009; Mavris et al. 2010; Dümig et al., 2011; Kabala & Zapart 2012; D'Amico et al., 2014; Li et al., 2018), China (He & Tang 2008), and high arctic regions (Nakatsubo et al., 1998; Bekku et al., 2004; Nakatsubo et al., 2005; Yoshitake et al., 2011; Osono et al., 2016). However, the increment in ecosystem carbon content was evident only in recently deglaciated terrain (T2), with an average increment of 9 g C m^{-2} y^{-1} in the ~150 years after deglaciation in the LIA moraine, while further C accumulation was negligible in the older successional stage (T3).

In a broader temporal perspective, we expect that, when the foreseen increase in temperature will become effective, forest vegetation will be able to establish and grow. In that case, the current limited capacity of accumulating carbon will be only transient, since forest vegetation is known for having larger and long-lasting capacity of accumulating carbon (Luyssaert et al., 2009).

While the differences in organic C accumulated aboveground were not significant, biomass in BG vegetation was significantly greater in older stages (T2 and T3) than in the early stage (Figure 5,

PeerJ Preprints | https://doi.org/10.7287/peerj.preprints.27703v1 | CC BY 4.0 Open Access | rec: 6 May 2019, publ: 6 May 2019

Table 2). These results suggest that the growth rate of BG parts in T3 ($p < 0.05$) and AG parts in T2 ($p > 0.05$) are considerable.

The deeper soil in older stages can partly account for the greater BG biomass compared to early stages, where the poor development of soil, extremely low air temperature, low soil moisture and short growing season might limit the accumulation of BG biomass (Chapin et al., 1992; Oechel & Billings, 1992; Osono et al., 2016). Therefore, BG parts of plants are almost negligible in the earlier stages of succession (Nakatsubo et al., 1998). Probably, the highest AG biomass, C and N in T2 is due to the greatest photosynthetic and carbon sink capacity that was observed in this stage.

The soil C and N content tended to increase along the chronosequence. Soil N reached the highest value in T3, but the difference with T2 was insignificant. The observed range of soil C and N was 40 to 557 g C m^{-2} and 22 to 59 g N m^{-2}, which were within the ranges reported by other studies in the deglaciated terrain (Egli et al., 2001; Dümig et al., 2012; Kabala & Zapart, 2012), and lower compared to amounts reported by He & Tang (2008), Burga et al. (2009); Mavris et al. (2010) and Yoshitake et al. (2011).

As expected, the highest values of C and N content were found in the top 5 cm of the soil profile, where the largest amount of organic matter from litter accumulates (Egli et al., 2001; Pei-qin et al., 2005; Kabala & Zapart, 2012; Vogel, 2013). In contrast to C and N, bulk density decreased with time since deglaciation and increased with soil depth as found in previous studies (e.g., Schrumpf et al., 2011). Similarly, other studies have reported a decrease in bulk density with time since deglaciation and an increase with soil depth, with accumulation of organic matter, the start of parent material alteration, increase in ion exchange capacity and the formation of weathering products (Egli et al., 2006; Bernasconi et al., 2011; Vilmundardóttir et al., 2015).

The linkage between soil and vegetation evolution and the observed biological fluxes

Plant C and soil organic carbon are in active exchange with the atmosphere and small changes in soil organic C stocks could have severe impacts on the global C cycle (Knops et al., 2009; Wen-Jie et al., 2011; Cong et al., 2014; Walter et al., 2016; Luo et al., 2017). In general, only a few features have been considered, such as the microbiological contribution to the carbon cycle (Egli et al., 2006; Bardgett et al., 2007; He & Tang, 2008; Mavris et al., 2010; Dümig et al., 2011; Guelland et al., 2012; Kabala & Zapart, 2012; Chae et al., 2016). A number of these studies found

PeerJ Preprints | https://doi.org/10.7287/peerj.preprints.27703v1 | CC BY 4.0 Open Access | rec: 6 May 2019, publ: 6 May 2019

a clear increase in the flux parameters with increasing ecosystem age, and advocated that to the increasing vegetation cover and plant productivity, the organic status (biomass, C and N) increasing after recent deglaciation chronosequences in the Alps (Matthews, 1993; Egli et al., 2001; Burga et al., 2009; D'Amico et al., 2014; Li et al., 2018), and high arctic regions (Nakatsubo et al., 1998; Bekku et al., 2004; Nakatsubo et al., 2005; Yoshitake et al., 2011). Further, these studies pointed out that the organic matter increased mainly within the uppermost part of the soil profile, and decreased with increasing depth, whilst, bulk density decreased with time since deglaciation (Egli et al., 2001; Pei-qin et al., 2005; Egli et al., 2006; Kabala & Zapart, 2012; Vilmundardóttir et al., 2015;. However, Wietrzyk et al. (2018) highlighted that vegetation cover is the main factor which affects soil properties during primary succession. Additionally, chemical soil properties and distance from the glacier foreground affect species distribution and vegetation cover.

In our study, we confirmed the increase in fluxes (GEE, Reco) and soil C and N only during the first period after deglaciation, while in the later stage most of the measured variables levelled off or even decreased. To test the linkage between soil and climate variables with observed fluxes, we applied a multiple linear regression to indicate the potential correlation between current ecosystem gas exchange and achieved level of soil evolution and overall carbon accumulation. The amplitude of NEE and GEE was positively correlated to BW in BG vegetation and soil C, however with a p-level between 0.1 and 0.05 for NEE. Air temperature was correlated with flux amplitude, but with significant level for Reco only. It is well established that Reco increases with temperature with an exponential (Q10) or an Arrhenius type function (Lloyd and Taylor, 1994; Uchida et al., 2002; Janssens et al., 2003) and also our developed model exhibited higher Reco with higher air temperature. We also know that the combination of biological and environmental variables enhances the accuracy of soil respiration modelling (Migliavacca et al., 2011; Scandellari et al., 2015).

Other variables were loosely related with fluxes, with below-significance correlation: In particular, we did not find significant correlation between AG N and biological fluxes and we found significant correlation between soil N and Reco only. This result can be partly explained by the non-linear response of biological fluxes to N. For instance, Peng et al. (2017) showed that gross ecosystem productivity, ecosystem respiration, and net ecosystem exchange all exhibited nonlinear

PeerJ Preprints | https://doi.org/10.7287/peerj.preprints.27703v1 | CC BY 4.0 Open Access | rec: 6 May 2019, publ: 6 May 2019

responses to increasing N additions. Furthermore, we should emphasize that much of the stored N in the observed vegetation type is presumably not directly used for the current year photosynthesis, but it represents conversely a long-term investment to enhance plant resilience to the frequent disturbances.

We found also that the different Raunkiaer classification of the different life forms is not adequate for understanding the different plant growth strategies and forecast the fluxes. In fact, we observed a convergence in plant allocation of organic biomass, irrespective to the Raunkiaer classification (Table 3). For instance, the dominant plant in T3, i.e. *Loiseleuria procumbens*, is a plant with large lignified underground tissue, although it is classified among Camaephytes based on its buds position. Interestingly, Caccianiga et al. (2006) found a switch in plant strategy types (Grime 1988) during primary succession leading from ruderal (R) to stress (S) strategy dominance. We hypothesize that the modest linkage between AG and BG N and observed biological fluxes reflects the dominance of ruderal behaviour in mid successional stages, while late successional stages with stress-tolerating strategists could have more investment in belowground structures reflected in nitrogen accumulation in plant reservoirs above and below ground in addition to the foliar N content. The linkage between plant properties, in particular AG N, is therefore weaker than what was found by Lopez-Blanco et al. 2018 in tundra ecosystems by analysing the leaf N content only.

Net production and accumulated biomass along an ecological succession gradient

Kimmins (1987) suggested that at the beginning of each seral stages, net productivity will generally increase until perhaps the middle or later part of the stage, then level off, and finally decline somewhat as a transition to the next stage occurs. This pattern was confirmed by our results. Conoid has started to develop earlier and thus can be considered as an older succession stage than LIA moraine, but despite this fact, our result revealed that net production and mean biomass accumulation peaked in the LIA moraine (Figure 7). This finding implies that carbon accumulation in the different stages of the primary succession on the Matsch glacier foreground (Alps, Italy) was not ruled only by time since deglaciation. Kimmins (1987) suggested that net productivity declines in the older ecosystem because later successional species have been selected during their evolution more for resilience to adverse conditions than for rapid growth.

PeerJ Preprints | https://doi.org/10.7287/peerj.preprints.27703v1 | CC BY 4.0 Open Access | rec: 6 May 2019, publ: 6 May 2019

These findings have to be placed in the broader context of recurrent disturbances common to periglacial areas, possibly affecting the spatial distribution and the timing of evolution of vegetation. This subject has been discussed by Burga et al. (2009), and they concluded that large-scale factors such as time since deglaciation, topography and disturbance (floods, rockfalls, avalanches), as well as small-scale factors such as grain size and water content of the substrate, micro-relief and micro-climate seem to be crucial for the development of vegetation and soil after deglaciation.

Conclusion

We found an average carbon accumulation along the glacier retreat chronosequence of 9 g m^{-2} y^{-1} in the first ≈150 years after deglaciation. The largest part of the carbon was accumulated in BG living organs. After that period, we did not observe significant further C accumulation.

NEE increased significantly moving from the site near the current glacier tongue (2800 m a.s.l.) to the site in the LIA moraine (2450 m a.s.l.). In the oldest site (2350 m a.s.l.), the maximal uptake was similar to the one of the LIA moraine, but the quantum yield was lower and Reco was higher.

We observed also a positive linkage between small-scale plant species richness and assimilation at low radiation intensity. Additionally, higher N in the biomass of the Hemicryptophyte life form was linked with higher Reco. The species richness was maximal at the intermediate stage of ecosystem development after glacier retreat. At this seral stage (≈150 years), the sink capacity exceeded that of the older ecosystem, not influenced by the glacier presence in the last centuries.

This study suggests a strong negative feedback mechanism in the response of global change, where recently established 'ruderal' plants *sensu* Grime (Grime, 1977; Caccianiga et al. 2006) rapidly expanding after glacier retreat, express a strong carbon sink capacity, therefore effectively counteracting the increasing levels of carbon dioxide concentration in the atmosphere. This high sink capacity is only transitory, since the older seral stage, where more stress-tolerating plants prevail, approaches the steady state condition.

PeerJ Preprints | https://doi.org/10.7287/peerj.preprints.27703v1 | CC BY 4.0 Open Access | rec: 6 May 2019, publ: 6 May 2019

References

ASTM (American Society for Testing and Material). 1992. Standard test method for specific gravity of soils (D 854-91). In 1992 annual book of ASTM standards, Section 4: Construction, Vol. 8: Soil and Rocks, Dimension Stone, Geosynthetics, ASTM, Philadelphia, Penn.

Bardgett RD, Richter A, Bol R, Garnett MH, Bäumler R, Xu X, Lopez-Capel E, Manning DAC, Hobbs PJ, Hartley IR, Wanek W. 2007. Heterotrophic microbial communities use ancient carbon following glacial retreat. Biology Letters 3(5): 487–490 Doi:10.1098/rsbl.2007.0242.

Barry RG. 2006. The status of research on glaciers and global glacier recession: a review. *Progress in Physical Geography* 30: 285–306.

Bekku YS, Nakatsubo T, Kume A, Koizumi H. 2004. Soil microbial biomass, respiration rate, and temperature dependence on a successional glacier foreland in Ny-Ålesund, Svalbard. *Arctic, Antarctic, and Alpine Research* 36: 395-399.

Bernasconi, S. M., Bauder, A., Bourdon, B., Brunner, I., Bunemann, E., Christl, I., et al., 2011. Chemical and biological gradients along the Damma glacier soil chronosequence, Switzerland. Vadose Zo. J. 10, 867–883. doi: 10.2136/vzj2010.0129.

Bradley J.A., Anesio A. M., and Arndt S. 2017, Microbial and Biogeochemical Dynamics in Glacier Forefields Are Sensitive to Century-Scale Climate and Anthropogenic Change. Frontiers in Earth Science, https://doi.org/10.3389/feart.2017.00026.

Burga CA, Bertil Krüsi B, Egli M, Wernli M, Elsener S, Ziefle M, Fischer T, Mavris C. 2009. Plant succession and soil development on the foreland of the Morteratsch glacier (Pontresina, Switzerland): Straight forward or chaotic?. *Flora* 205: 561–576.

Caccianiga M, Luzzaro A, Pierce S, Ceriani RM, Cerabolini B, 2006. The functional basis of a primary succession resolved by CSR classification. *Oikos* 112: 10-20.

Chae N, Kang H., Kim Y., Hong SG, Lee BY, Choi T., 2015. CO2 efflux from the biological soil crusts of the High Arctic in a later stage of primary succession after deglaciation, Ny-Ålesund, Svalbard, Norway. Applied Soil Ecology, 98, DOI: 10.1016/j.apsoil.2015.09.013.

PeerJ Preprints | https://doi.org/10.7287/peerj.preprints.27703v1 | CC BY 4.0 Open Access | rec: 6 May 2019, publ: 6 May 2019

Chapin FS, Jefferies RL, Reynolds JF, Shaver GR, Svoboda J. 1992. *Arctic ecosystems in a changing climate. An ecophysiological perspective*. London: Academic Press.

Cong WF, Ruijven JV, Mommer L, Deyn GBD, Berendse F, Hoffland E. 2014. Plant species richness promotes soil carbon and nitrogen stocks in grasslands without legumes. *Journal of Ecology* 102: 1163–1170.

D'Amico ME, Freppaz M, Filippa C, Zanini E. 2014. Vegetation influence on soil formation rate in a proglacial chronosequence (Lys Glacier, NW Italian Alps). *Catena* 113:122–137.

Dalla Fior G. 1981. *La nostra flora*. Monauni, Trento.

Desai A,. Wohlfahrt G, Zeeman MJ, Katata G, Eugster W, Montagnani L, Gianelle D, Mauder M, Schmid HP. 2016. Montane ecosystem productivity responds more to global circulation patterns than climatic trends. *Environmental Research Letters* 11 (2): pii 024013 doi: 10.1088/1748-9326/11/2/024013.

Dümig A, Smittenberg R, Kögel-Knabner I. 2011. Concurrent evolution of organic and mineral components during initial soil development after retreat of the Damma glacier, Switzerland. *Geoderma* 163: 83–94.

Egli M, Fitze P, Mirabella A. 2001. Weathering and evolution of soils formed on granitic, glacial deposits: results from chronosequences of Swiss alpine environments. *Catena* 45: 19–47.

Egli M, Wernli M, Kneisel C, Haeberli W. 2006. Melting Glaciers and Soil Development in the Proglacial Area Morteratsch (Swiss Alps): I. Soil Type Chronosequence. *Arctic, Antarctic, and Alpine Research* 38(4):499-509.

Eugster W., Moffat, A M., Ceschia, E., Aubinet M., Ammann C., Osborne B., Davis PA., Smith P., Jacobs C., Moors E., Le Dantec V., Béziat P., Saunders M., Jans W., Grünwald T., Rebmann C., Kutsch W L., Czerný R., Janous D., Moureaux C., Dufranne D., Carrara A., Magliulo V., Di Tommasi P., Olesen J. E., Schelde K., Olioso A., Bernhofer C., Cellier P., Larmanou E., Loubet B., Wattenbach M., Marloie O., Sanz,M.-J., Søgaard H. , Buchmann N. 2010. Management effects on European cropland respiration. Agriculture, Ecosystems & Environment, 139, (3), 2010, 346-362. (DOI): 10.1016/j.agee.2010.09.001.

PeerJ Preprints | https://doi.org/10.7287/peerj.preprints.27703v1 | CC BY 4.0 Open Access | rec: 6 May 2019, publ: 6 May 2019

Field C, Mooney HA. 1986. The photosynthesis-nitrogen relationship in wild plants. In: Givinsh TJ (ed) On the economy of form and function. Cambridge: Cambridge University Press.

Forzieri G., Alkama R., Miralles DG, Cescatti A. 2017. Satellites reveal contrasting responses of regional climate to the widespread greening of Earth. Science. 16;356(6343):1180-1184. doi: 10.1126/science.aal1727.

Frey W, Frahm JP, Fischer E, Lobin W. 2006. *Liverworts, Mosses and Ferns of Europe*. Colchester: Harley Books.

Galvagno, M., Wohlfahrt, G., Cremonese, E., Filippa, G., Migliavacca, M., di Cella, U.M., van Gorsel, E., 2017. Contribution of advection to nighttime ecosystem respiration at a mountain grassland in complex terrain. Agric. For. Meteorol. 237–238, 270–281. https://doi.org/10.1016/j.agrformet.2017.02.018.
http://www.sciencedirect.com/science/article/pii/S0168192317300515.

Grime JP. 1977. Evidence for the existence of three primary strategies in plants and its relevance to ecological and evolutionary theory. The American Naturalist 111:1169–1194.

Grime JP, Hodgson JG, Hunt R.1988. Comparative plant ecology, A Functional Approach to Common British Species. Springer Science-Business media, Dordrecht.

Guelland K., Hagedorn F, Smittenberg RH, Goransson H, Bernasconi SM, Hajdas I, Kretzschmar R. 2012. Evolution of carbon fluxes during initial soil formation along the forefield of Damma glacier, Switzerland. *Biogeochemistry* 113:545–561.

Habler G, Thöni M, Grasemann B. 2009. Cretaceous metamorphism in the Austroalpine Matsch Unit (Eastern Alps): the interrelation between deformation and chemical equilibration processes. *Miner Petrol* 97:149–171 Doi:10.1007/s00710-009-0094-x.
He L, Tang Y. 2008. Soil development along primary succession sequences on moraines of Hailuogou Glacier, Gongga Mountain, Sichuan, China. *Catena* 72: 259–269.

Huff LM, Potts DL, Hamerlynck EP. 2015. Ecosystem CO_2 exchange in response to nitrogen and phosphorus addition in a restored, temperate grassland. *The American Midland Naturalist* 173(1):73-87.

PeerJ Preprints | https://doi.org/10.7287/peerj.preprints.27703v1 | CC BY 4.0 Open Access | rec: 6 May 2019, publ: 6 May 2019

Kabala C, Zapart J. 2012. Initial soil development and carbon accumulation on moraines of the rapidly retreating Werenskiold Glacier, SW Spitsbergen, Svalbard archipelago. *Geoderma* 175–176: 9–20.

Kimmins JP. 1987. *Forest ecology*., London: Macmillan Publishing Company Press.

Kozioł K, Ruman M, Kozak K, Polkowska Z. 2014. Release and Transport of Toxic, Mobile Organic Compounds (Formaldehyde and Phenols) on an Arctic Glacier. *APCBEE Procedia* 10: 16 – 20.

Knoll C, Kerschner H. 2009. A glacier inventory for South Tyrol, Italy, based on airborne laserscanner data. *Annals of Glaciology* 50 (53): 46–52 Doi:10.3189/172756410790595903.

Knops JMH, Bradley KL. 2009. Soil carbon and nitrogen accumulation and vertical distribution across a 74-year chronosequence. *Soil Science Society of America Journal* 73: 2096-2104.

Kutzbach L, Schneider J, Sachs T, Giebels M, Nykänen H, Shurpali NJ, Martikainen P J, Alm J, Wilmking M. 2007. CO2 flux determination by closed-chamber methods can be seriously biased by inappropriate application of linear regression. Biogeosciences 4: 1005–1025 Doi:10.5194/bg-4-1005-2007.

Janssens I.A., Dore S., Epron D., Lankreijer H., Buchmann N., Longdoz B., Brossaud J., Montagnani L. (2003). Climatic influences on seasonal and spatial differences in soil CO2 efflux. In: Canopy fluxes of energy, water and carbon dioxide of European forests / Valentini R. [edit.], Berlin, Ecological Studies, Springer. Pp. 235-256.

Leuschner CJ.,Ellenberg H. Ecology of Central European Forests. Springer International Publishing 2017, DOI:10.1007/978-3-319-43048-5.

Li Q, Jia Z, Feng L, He L,Yang K. 2018. Dynamics of biomass and carbon sequestration across a chronosequence of Caragana intermedia plantations on alpine sandy land. *Scientific Reports* 8 (12432): 1-9.

Liang J., T.W. Crowther, N. Picard, S. Wiser, Mo Zhou, G.Alberti, E.-D.Schulze, et al., 2016, Positive biodiversity-productivity relationship predominant in global forests. Science 354, aaf8957, DOI: 10.1126/science.aaf8957.

PeerJ Preprints | https://doi.org/10.7287/peerj.preprints.27703v1 | CC BY 4.0 Open Access | rec: 6 May 2019, publ: 6 May 2019

Li-Cor, 2010. Li-8100a Automated Soil CO2 Flux System & Li-8150 Multiplexer Instruction Manual.

Lloyd J, Taylor J. 1994. On the temperature dependence of soil respiration. *Functional Ecology* 8: 315–323.

López-Blanco, E., Lund, M., Christensen, T. R., Tamstorf, M. P., Smallman, T. L., Slevin, D., et al. (2018). Plant traits are key determinants in buffering the meteorological sensitivity of net carbon exchanges of Arctic tundra. Journal of Geophysical Research: Biogeosciences, 123, 2675–2694. https://doi.org/10.1029/2018JG004386.

Luo W, Li MH, Sardans J, Lü XT, Wang C, Peñuelas J, Wang Z, Han XG, Jiang Y. 2017. Carbon and nitrogen allocation shifts in plants and soils along aridity and fertility gradients in grasslands of China. *Ecology and Evolution* 7: 6927–6934.

Luyssaert S., E.–D. Schulze, A. Börner, A. Knohl, D. Hessenmöller, B. E. Law, P. Ciais & J. Grace, 2008, Old-growth forests as global carbon sinks, Nature, doi:10.1038/nature07276.

Matthews JA, 1992. *The Ecology of Recently Deglaciated Terrain. A Geoecological Approach to Glacier Forelands and Primary Succession.* Cambridge: Cambridge University Press.

Mavris C, Egli M, Ploetze M, Blum JD, Mirabella A, Giaccai D, Haeberli W. 2010. Initial stages of weathering and soil formation in the Morteratsch proglacial area (Upper Engadine, Switzerland). *Geoderma* 155: 359–371.

Metcalfe DB, Fisher RA, Wardle, DA, 2011. Plant communities as a driver of soil respiration. Biogeosciences : pathways, mechanisms, and significance for global change Biogeosciences, 8, 2047-2061, 2011, https://doi.org/10.5194/bg-8-2047-2011

Migliavacca M., M. Reichstein, A.D. Richardson, R. Colombo, M.A. Sutton, G. Lasslop, E. Tomelleri, G. Wohlfahrt, N. Carvalhais, A. Cescatti, M.D. Mahecha, L. Montagnani, D. Papale, S. Zaehle, A. Arain, A. Arneth, T.A. Black, A. Carrara, S. Dore, D. Gianelle, C. Helfter, D. Hollinger, W.L. Kutsch, P-M. Lafleur, Y. Nouvellon, C. Rebmann, R. Humberto, M. Rodeghiero, O. Roupsard, M. Sebastià., G. Seufert, J. Soussana, K. Michiel (2011). Semiempirical modeling of abiotic and biotic factors controlling ecosystem respiration across eddy covariance sites. Global Change Biology, 17(1), 390-409. DOI: 10.1111/j.1365-2486.2010.02243.x.

PeerJ Preprints | https://doi.org/10.7287/peerj.preprints.27703v1 | CC BY 4.0 Open Access | rec: 6 May 2019, publ: 6 May 2019

Moffat AM. 2012. A new methodology to interpret high resolution measurements of net carbon fluxes between the terrestrial ecosystems and the atmosphere. Doctoral dissertation. Friedrich-Schiller-Universität Jena.

Nakatsubo T, Bekku Y, Kume A, Koizumi H. 1998. Respiration of the belowground parts of vascular plants: its contribution to total soil respiration on a successional glacier foreland in Ny-Alesund, Svalbard. *Polar Rererirch* 17(1), 53-59.

Nakatsubo T, Bekku YS, Uchida M, Muraoka H, Kume A, Ohtsuka T, Masuzawa T, Kanda H, Koizumi H. 2005. Ecosystem development and carbon cycle on a glacier foreland in the high Arctic, Ny-Ålesund, Svalbard. *Journal of Plant Research* 118:173–179.

Odum EP. 1969. The Strategy of Ecosystem Development. *Science* 164: 262-270.

Oechel WC, Billings WD. 1992. Effects of global change on the carbon balance of arctic plants and ecosystems. In: Chapin FS, Jefferies RL, Reynolds JF, Shaver GR, Svoboda J (Eds.), *Arctic Ecosystems in a Changing Climate, an Ecophysiological Perspective*. London: Academic Press.

Oechel WC, Vourlitis G. 1994. The effects of climate charge on land-atmosphere feedbacks in arctic tundra regions. *Trends in ecology & evolution* 9 (9): 324-329, Doi:10.1016/0169-5347(94)90152-X.

Osono T., Mori AS., Uchida M. Kanda H., 2016. Accumulation of carbon and nitrogen in vegetation and soils of deglaciated area in Ellesmere Island, high-Arctic Canada. Polar Science 10(3) 288-296, http://dx.doi.org/10.1016/j.polar.2016.03.003.

Pavelka M., M. Acosta, R. Kiese, N. Altimir, C. Brümmer, P. Crill, E. Darenova, R. Fuß, B. Gielen, A. Graf, L. Klemedtsson, A. Lohila, B. Longdoz, A. Lindroth, M. Nilsson, S. Marañon-Jimenez, L. Merbold, L. Montagnani, M. Peichl, M. Pihlatie, J. Pumpanen, P. Serrano Ortiz, H. Silvennoinen, U. Skiba, P. Vestin, P. Weslien, D. Janouš, W. Kutsch, 2018. Standardisation of chamber technique for CO2, N2O and CH4 fluxes measurements from terrestrial ecosystems, International Agrophysics 32, 569-587, DOI: 10.1515/intag-2017-0045.

Pei-qin P., Wen-ju Z., Cheng T., Xiao – li W, Chang-an C. 2005. Soil C, N and P contents and their relationships with soil physical properties in wetlands of Dongting Lake floodplain. *Journal of Soil and Water Conservation* 19 (1): 49-53.

PeerJ Preprints | https://doi.org/10.7287/peerj.preprints.27703v1 | CC BY 4.0 Open Access | rec: 6 May 2019, publ: 6 May 2019

Peng Y, Li F, Zhou G, Fang K, Zhang D, Li C, Yang G, Wang G, Wang J, Yang Y. 2017. Linkages of plant stoichiometry to ecosystem production and carbon fluxes with increasing nitrogen inputs in an alpine steppe. *Global Change Biology* 23:5249–5259.

Penna D, Engel M, Mao L, Dell'Agnese A, Bertoldi G, Comiti F. 2014.Tracer-based analysis of spatial and temporal variations of water sources in a glacierized catchment. *Hydrology and Earth System Sciences* 18: 5271–5288 Doi:10.5194/hess-18-5271-2014.

Pepin N, Bradley RS, Diaz HF. et al. 2015. Elevation dependent warming in mountain regions of the world. *Nature Climate Change* 5: 424–430, https://doi.org/10.1038/nclimate2563

Raunkiaer CC, 1934. The Life Forms of Plants and Statistical Plant Geography, Oxford, Oxford University Press.

Reich PB, Tjoelker MG, Machado J-L & Jacek Oleksyn J., 2006. Universal scaling of respiratory metabolism, size and nitrogen in plants. Nature, 439, 457–461, doi:10.1038/nature04282.

Reich PB, 2014. The world-wide 'fast–slow' plant economics spectrum: a traits manifesto. Journal of Ecology 2014, 102, 275–301 doi: 10.1111/1365-2745.12211.

Running, S. W. and S. T. Gower (1991): "FOREST-BGC, A general model of forest ecosystem processes for regional applications. II. Dynamic carbon allocation and nitrogen budgets.", Tree Physiol 9(1-2): 147-160.

Scandellari, F.; Zanotelli, D.; Ceccon, C.; Bolognesi, M.; Montagnani, L.; Cassol, P.; Melo, G. W.; Tagliavini, M., 2015., Enhancing prediction accuracy of soil respiration in an apple orchard by integrating photosynthetic activity into a temperature-related model, European Journal of Soil Biology, 70, 77-87. Doi: 10.1016/j.ejsobi.2015.07.006

Schmitt M, Bahn M, Wohlfahrt G, Tappeiner U, Cernusca A. 2010. Land use affects the net ecosystem CO2 exchange and its components in mountain grasslands. *Biogeosciences* 7:2297–2309 Doi:10.5194/bg-7-2297-2010.

Schrumpf M., Schulze E. D., Kaiser K., and Schumacher,J.2011. How accurately can soil organic carbon stocks and stock changes be quantified by soil inventories? Biogeosciences, 8, 1193-1212, https://doi.org/10.5194/bg-8-1193-2011.

PeerJ Preprints | https://doi.org/10.7287/peerj.preprints.27703v1 | CC BY 4.0 Open Access | rec: 6 May 2019, publ: 6 May 2019

Song B, Sun J, Zhou Q, Zong N, Li L, Niu S.2017. Initial shifts in nitrogen impact on ecosystem carbon fluxes in an alpine meadow: patterns and causes. Biogeosciences 14: 3947–3956.

Sigl M., Abram N.J., Gabrieli J., Jenk T.M., Dimitri Osmont D., and Schwikowski M., 2018, 19th century glacier retreat in the Alps preceded the emergence of industrial black carbon deposition on high-alpine glaciers. The Cryosphere, 12, 3311-3331, https://doi.org/10.5194/tc-12-3311-2018.

Smith CW, Aptroot A, Coppins BJ, Fletcher A, Gilbert OL, James PW, Wolseley PA (eds). 2009. *The lichens of Great Britain and Ireland*. London: British Lichen Society, Department of Botany, The Natural History Museum, London, UK.

Solomina O.N., R.S. Bradley , V. Jomelli, A. Geirsdottir , D. S. Kaufman, J. Koch, N. P. McKay , M. Masiokas, G. Miller, A. Nesje, K. Nicolussi, L.A. Owen, A.E. Putnam, H. Wanner, G. Wiles, B.Yang (2016) Glacier fluctuations during the past 2000 years Quaternary Science Reviews 149 (2016) 61e90.

Tanga Z, Xub W, Zhouc G, Baib Y, Lib J, Tang X, Chen D, Liu Q, Ma W, Xiong G, He H, He N, Guo Y, Guo Q, Zhu J, Han W, Hu H, Fang J, Xie Z. 2018. Patterns of plant carbon, nitrogen, and phosphorus concentration in relation to productivity in China's terrestrial ecosystems. *PNAS* 115 (16) 4033–4038.

Thornton, P. E. and N. A. Rosenbloom, 2005. Ecosystem model spin-up: Estimating steady state conditions in a coupled terrestrial carbon and nitrogen cycle model. Ecological Modelling 189 (1-2): 25-48.

Uchida M, Muraoka H, Nakatsubo T, Bekku Y, Ueno T, Kanda H, Koizumi H. 2002. Net Photosynthesis, Respiration, and Production of the Moss Sanionia uncinata on a Glacier Foreland in the High Arctic, Ny-Ålesund, Svalbard. *Arctic, Antarctic, and Alpine Research* 34 (3): 287-292.

Uchida M, Nakatsubo T, Kanda H, Koizumi H. 2006. Estimation of the annual primary production of the lichen Cetrariella delisei in a glacier foreland in the High Arctic, Ny-Ålesund, Svalbard. *Polar Research* 25(1): 39–49.

Varolo E, Zanotelli D, Montagnani L, Tagliavini M, Zerbe S. 2016. Colonization of a Deglaciated Moraine: Contrasting Patterns of Carbon Uptake and Release from C3 and CAM Plants. *PLosOne,* 11(12): e0168741. doi:10.1371/journal.pone.0168741.

PeerJ Preprints | https://doi.org/10.7287/peerj.preprints.27703v1 | CC BY 4.0 Open Access | rec: 6 May 2019, publ: 6 May 2019

Vilmundardóttir OK, Gísladóttir G, Lal R. 2015. Between ice and ocean; soil development along an age chronosequence formed by the retreating Breiðamerkurjökull glacier, SE-Iceland. *Geoderma* 259–260: 310–320.

Vogel E. 2013. The temporal and spatial variability of soil respiration in boreal forests - A case study of Norunda forest, Central Sweden. Master thesis.

Walker LR, Del Moral R. 2003. *Primary succession and ecosystem rehabilitation.* Cambridge: Cambridge University Press, Cambridge, UK.

Walker LR, Del Moral R. 2011. Primary Succession. In: eLS. John Wiley & Sons, Ltd: Chichester. DOI: 10.1002/9780470015902.a0003181.pub2

Waide RB,, M. R. Willig, C. F. Steiner, G. Mittelbach, L. Gough, S. I. Dodson, G.P. Juday and R. Parmenter. 1999. The Relationship between Productivity and Species Richness. Annual Review of Ecology and Systematics, 30 257-300.

Walter K, Don A, Tiemeyer B, Freibauer A. 2016. Determining Soil Bulk Density for Carbon Stock Calculations: A Systematic Method Comparison. *Soil Science Society of America Journal* 80: 579–591.

Wang Y, Jiang Q, Yang Z, Sun W, Wang D. 2015. Effects of water and nitrogen addition on ecosystem carbon exchange in a meadow steppe. PLoS ONE 10 (5): e0127695, Doi:10.1371/journal.pone.0127695

Wen-Jie W, Ling Q, Yuan - Gang Z, Dong-Xue S, Jing A, Hong-Yan W, Guan-Yu Z, Wei S, Xi-Quan C. 2011. Changes in soil organic carbon, nitrogen, pH and bulk density with the development of larch (Larix gmelinii) plantations in China. *Global Change Biology*. 1-20. doi: 10.1111/j.1365-2486.2011.02447.x

Wirth V, Hauck M, Schultz M (eds). 2013. *Die Flechten Deutschlands*. Stuttgart: Ulmer, DE.

Wietrzyk P, Rola K, Osyczka P, Nicia P, Szymański W, Węgrzyn M. 2018. The relationships between soil chemical properties and vegetation succession in the aspect of changes of distance from the glacier forehead and time elapsed after glacier retreat in the Irenebreen foreland (NW Svalbard). *Plant Soil* 428:195–211.

PeerJ Preprints | https://doi.org/10.7287/peerj.preprints.27703v1 | CC BY 4.0 Open Access | rec: 6 May 2019, publ: 6 May 2019

Wirth, V, Hauck M, and M. Schulz. 2013. Die Flechten Deutschlands, Eugen Ulmer, Stuttgart. DE.

Xia J, Niu S, Wan S. 2009. Response of ecosystem carbon exchange to warming and nitrogen addition during two hydrologically contrasting growing seasons in a temperate steppe. *Global Change Biology 15*: 1544–1556, Doi: 10.1111/j.1365-2486.2008.01807.x

Yoshitake S, Uchida M, Koizumi H, Nakatsubo T. 2007. Carbon and nitrogen limitation of soil microbial respiration in a High Arctic successional glacier foreland near Ny-Ålesund, Svalbard. *Polar Research* 26: 22–30.

Yoshitake S, Uchida M, Ohtsuka T, Kanda H, Koizumi H, Nakatsubo T. 2011. Vegetation development and carbon storage on a glacier foreland in the High Arctic, Ny-Alesund, Svalbard. *Polar Science* 5: 391-397.

Zangheri P. 1976. *Flora Italica*. CEDAM. Padova.

Zemp M, H. Frey, I. Gärtner-Roer et al., Historically unprecedented global glacier decline in the early 21st century. Journal of Glaciology, Vol. 61, No. 228, 2015 doi: 10.3189/2015JoG15J017.

Zhao P., A. Hammerle, M. Zeeman, G. Wohlfahrt, 2018. On the calculation of daytime CO2 fluxes measured by automated closed transparent chambers, Agricultural and Forest Meteorology 263 (2018) 267–275, https://doi.org/10.1016/j.agrformet.2018.08.022.

PeerJ Preprints | https://doi.org/10.7287/peerj.preprints.27703v1 | CC BY 4.0 Open Access | rec: 6 May 2019, publ: 6 May 2019

Figures

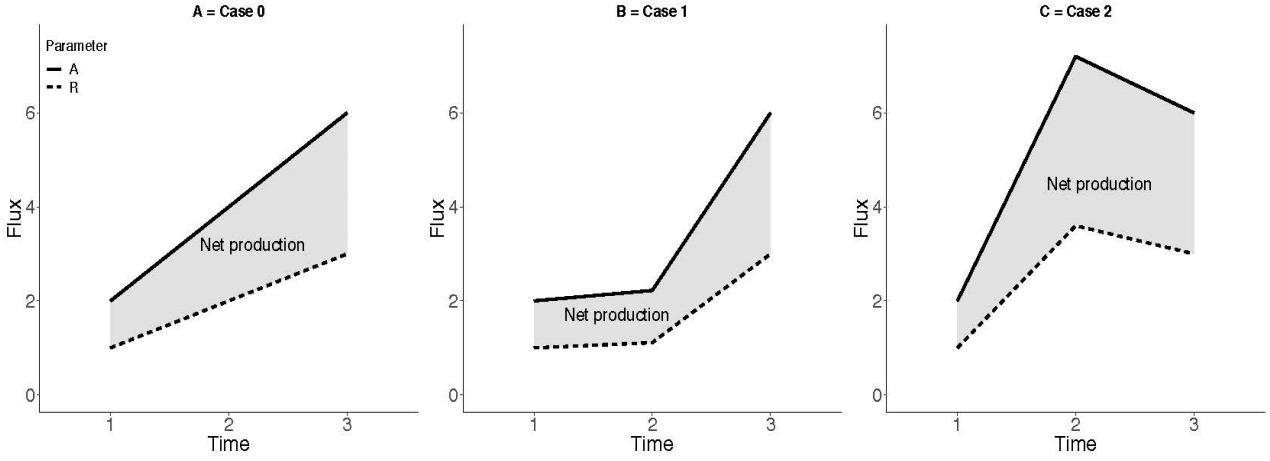

Figure 1

A conceptual representation of the development of a primary succession.

(A) In Case 0, photosynthesis (A) and respiration (R) increase linearly. (B) In Case 1, photosynthesis and respiration increase less than linearly in the intermediate stage. (C) In Case 2, photosynthesis and respiration peak occur in the intermediate stage.

PeerJ Preprints | https://doi.org/10.7287/peerj.preprints.27703v1 | CC BY 4.0 Open Access | rec: 6 May 2019, publ: 6 May 2019

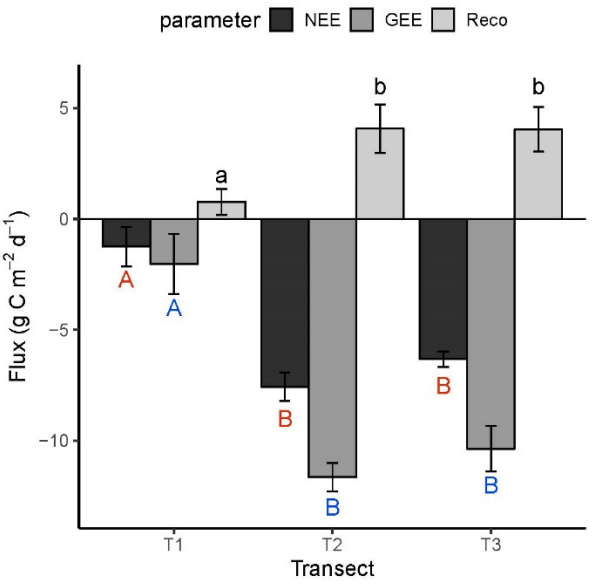

Figure 2

The mean daily value of NEE, GEE, and Reco in the different transects. Reco - ecosystem respiration, GEE- gross primary productivity, NEE - net ecosystem exchange. Each value is the mean of three campaigns with standard deviation (SD).

Statistical significance between transect indicates with lowercase letters for Reco, red capital letters for NEE and blue capital letters for GEE. The different letters are indicating significant differences between transects according to ANOVA test.

PeerJ Preprints | https://doi.org/10.7287/peerj.preprints.27703v1 | CC BY 4.0 Open Access | rec: 6 May 2019, publ: 6 May 2019

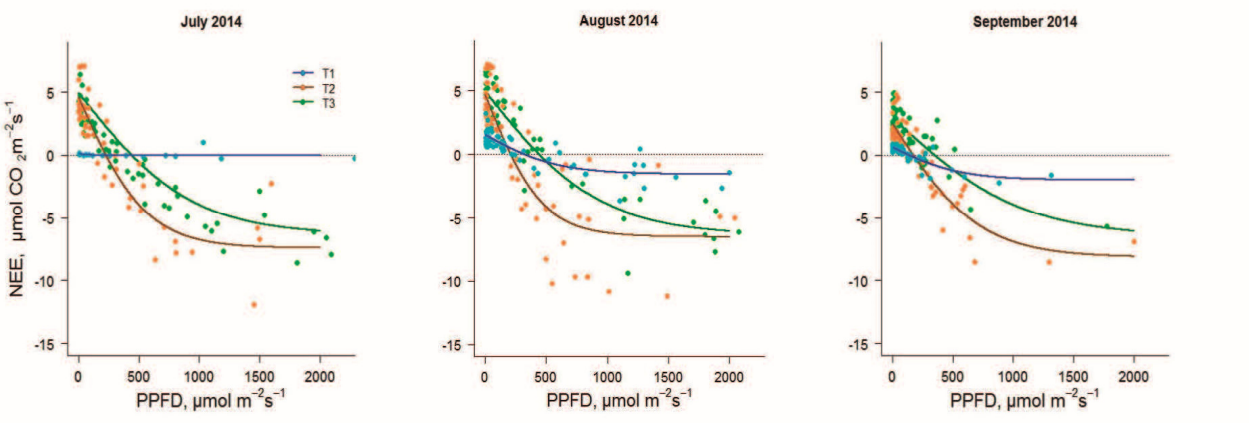

Figure 3

Light response curves between PAR and NEE in the three transects (T1 - glacier 2800 m,T2 - LIA moraine 2450 m, T3 - conoid 2350 m) in the months of July, August, and September 2014. (A) July. (B) August. (C) September. NEE - net ecosystem exchange, PPFD – photosynthetic photon flux density.

PeerJ Preprints | https://doi.org/10.7287/peerj.preprints.27703v1 | CC BY 4.0 Open Access | rec: 6 May 2019, publ: 6 May 2019

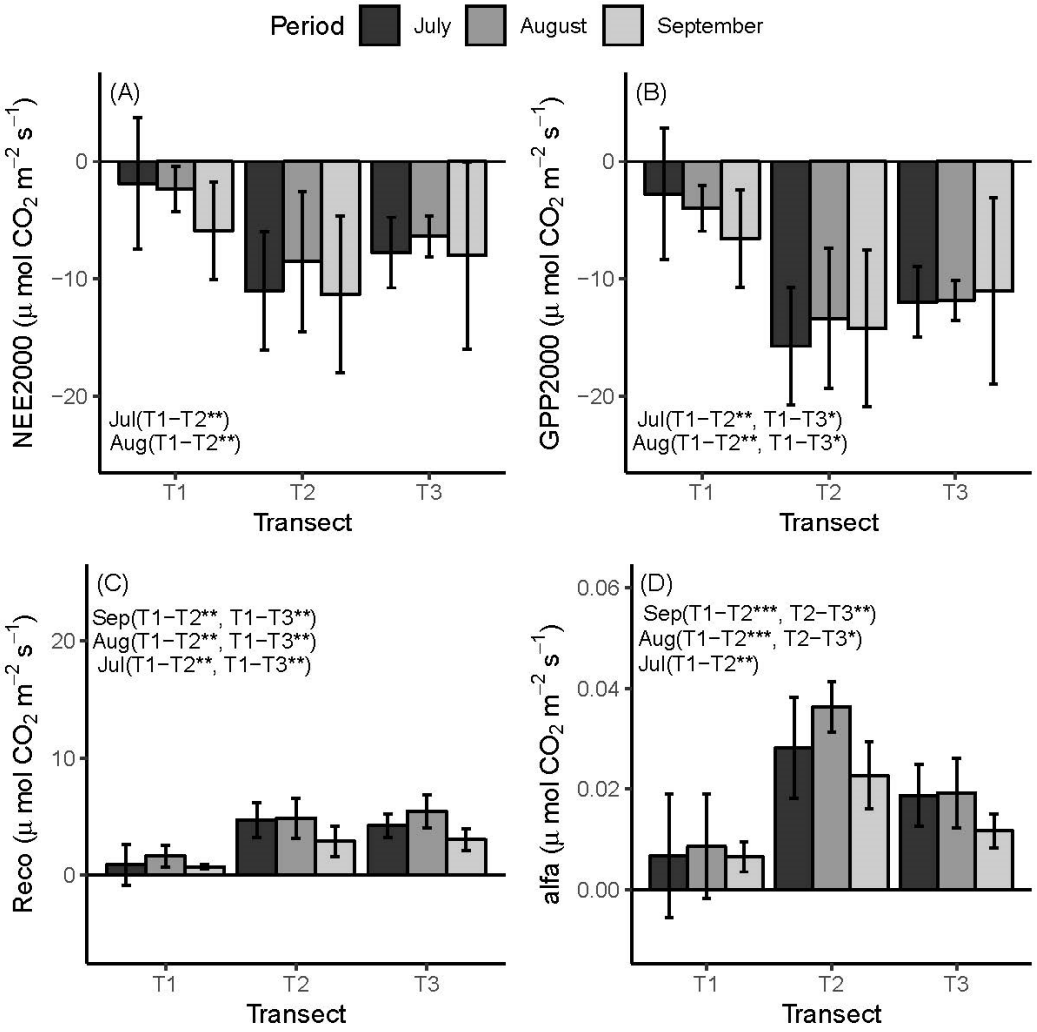

Figure 4

Mean flux parameters at the three transects during the field campaigns.

(A) Mean NEE2000. (B) GEE2000. (C) Reco at a reference temperature of 10 °C (R10). (D) alfa. NEE2000 - net ecosystem exchange at the PPFD of 2,000 µmol m-2 s-1; GEE2000 – gross primary productivity at the photosynthetic active photon flux density (PPFD) of 2,000 µmol m^{-2} s^{-1}; Reco - ecosystem respiration; alfa - the quantum yield in the light response curve. Negative values indicate net CO2 uptake and positive values represent net released CO2 to the atmosphere. T1 = glacier 2800 m, T2 = LIA moraine 2450 m, T3 = conoid 2350 m. Asterisks indicate significance levels: * $p \leq 0.05$, ** $p \leq 0.01$, *** $p \leq 0.001$.

PeerJ Preprints | https://doi.org/10.7287/peerj.preprints.27703v1 | CC BY 4.0 Open Access | rec: 6 May 2019, publ: 6 May 2019

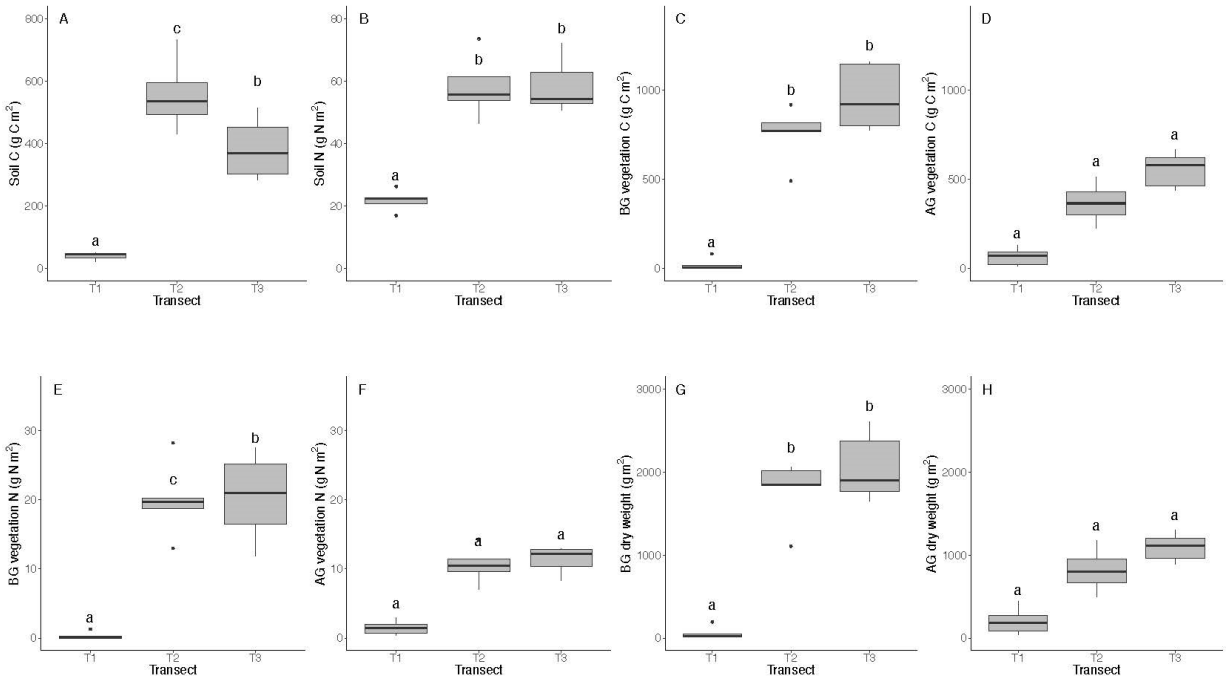

Figure 5

Boxplots showing the results of soil and vegetation analyses.

(A) Soil carbon. (B) Soil nitrogen. (C) Carbon in BG vegetation. (D) Carbon in AG vegetation. (E) Nitrogen in BG vegetation. (F) Nitrogen in AG vegetation. (G) BG biomass. (H) AG biomass. Lowercase letters indicate the results of statistical tests with different letters indicating significant differences between transects (BG – belowground, AG – aboveground).

PeerJ Preprints | https://doi.org/10.7287/peerj.preprints.27703v1 | CC BY 4.0 Open Access | rec: 6 May 2019, publ: 6 May 2019

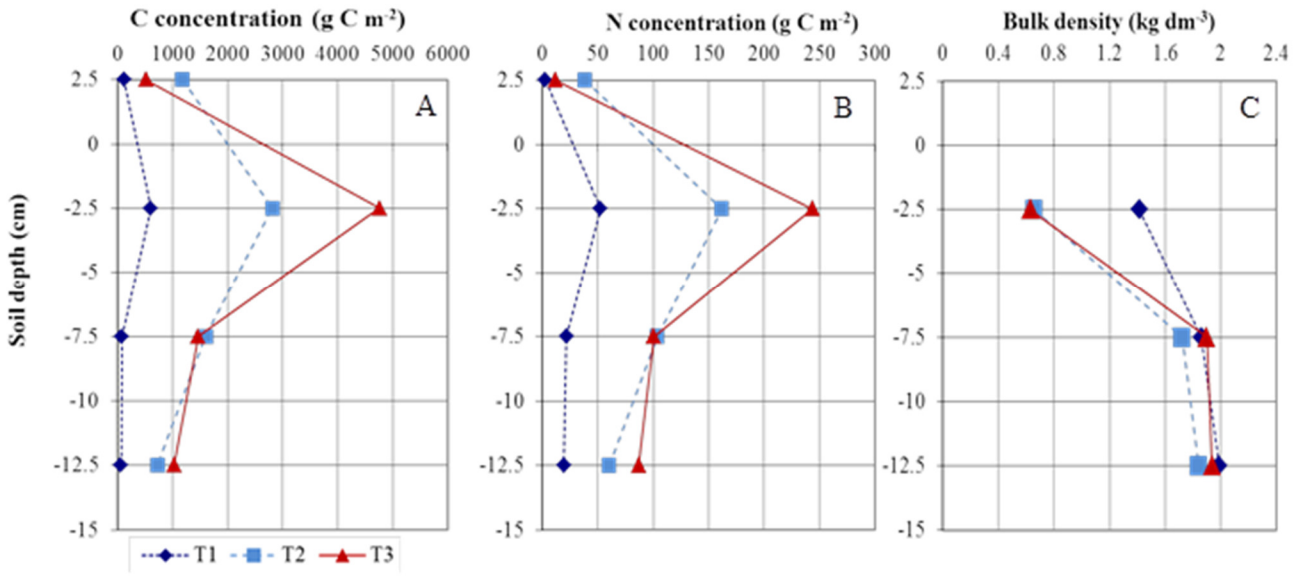

Figure 6

Average vertical profiles of carbon, nitrogen and bulk density in the three transects.

(A) Carbon. (B) Nitrogen (C) Soil bulk density. Average values in the different depths (±2.5 cm) of the soil profile.

PeerJ Preprints | https://doi.org/10.7287/peerj.preprints.27703v1 | CC BY 4.0 Open Access | rec: 6 May 2019, publ: 6 May 2019

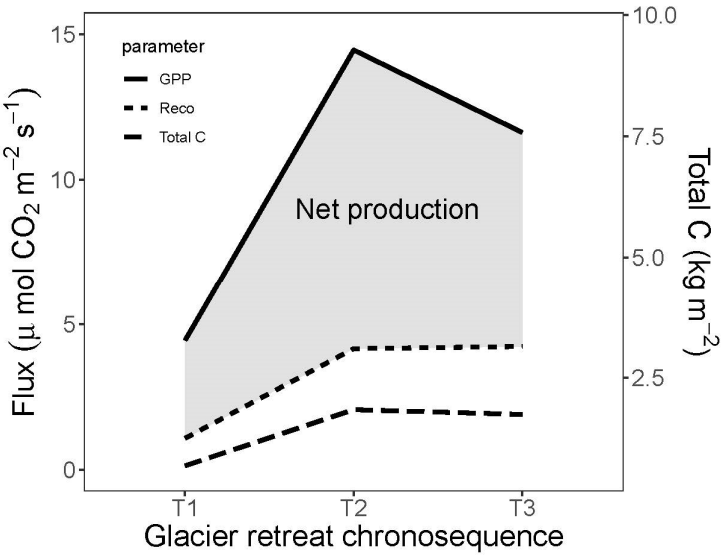

Figure 7

Schematic illustration of the net production and total C along the glacier retreat chronosequence.

Net production (µmol m-2s-1) and total C (mean accumulated carbon in AG and BG vegetation + soil carbon (kg m-2), along the glacier retreat chronosequence. GPP – gross primary production = - GEE; Reco – ecosystem respiration; T1 - glacier 2800 m, T2 - LIA moraine 2450 m; T3 - conoid 2350 m).

PeerJ Preprints | https://doi.org/10.7287/peerj.preprints.27703v1 | CC BY 4.0 Open Access | rec: 6 May 2019, publ: 6 May 2019

Tables

Table 1

Plant species composition in the different transect.

Different transects (T1: T3) and different collars in each transect (C1: C5). Plant taxa: B=Bryophytes; D=Dycotyledons; L=Lichens; M=Monocotyledons. Life forms: C= Camaephyte; G=Geophyte; H=Hemicryptophyte; T=Therophyte.

Plant species	**Taxo-nomic group**	**Life form**	**T1**					**T2**					**T3**				
			C1	C2	C3	C4	C5	C1	C2	C3	C4	C5	C1	C2	C3	C4	C5
Arenaria biflora L	*M*	*C*									+						
Cardamine resedifolia L.	*D*	*H*							+					+			+
Cerastium cerastioides (L.) Britton	*D*	*C*									+						
Euphrasia rostkoviana Hayne	*D*	*T*						+		+		+				+	
Festuca halleri All.	*M*	*H*						+	+	+	+	+	+	+		+	
Flavocetraria cucullata (Bellardi) Kärnefelt & A.Thell	*L*																+
Gentiana acaulis L.	*D*	*H*							+			+					
Loiseleuria procumbens (L.) Desv.	*D*	*C*											+	+	+	+	+
Lotus alpinus (DC.) Ramond	*D*	*H*						+		+	+	+				+	
Luzula alpino-pilosa (Chaix) Breistr.	*M*	*H*						+					+	+	+		
Nardus stricta L.	*M*	*H*								+							
Poa laxa Haenke	*M*	*H*	+	+		+	+										
Pohlia filum (Schimp.) Martensson	B		+	+	+	+	+										
Potentilla erecta (L.) Räusch.	*D*	*H*								+			+	+	+	+	+
Pulsatilla vernalis (L.) Mill.	*D*	*G, H*											+		+	+	
Racomitrium canescens (Hedw.) Brid.	*B*							+	+	+	+	+					
Sibbaldia procumbens L.	*D*	*H*							+	+	+						
Soldanella alpina L.	*D*	*H*												+	+		+
Trifolium alpinum L.	*D*	*H*							+								
Total number of plant species in each collar			2	2	1	2	2	5	6	7	6	5	5	6	5	6	5
Total number of plant species in each transect			2					13					10				

PeerJ Preprints | https://doi.org/10.7287/peerj.preprints.27703v1 | CC BY 4.0 Open Access | rec: 6 May 2019, publ: 6 May 2019

Table 2

Accumulated carbon and nitrogen in soil, roots and AG vegetation (g m^{-2}) in each transect.

T1 - glacier 2800 m, T2 - LIA moraine 2450 m, T3 - conoid 2350 m, ± SD - standard deviation, AG – aboveground, BG- belowground, asterisks * - $p \leq 0.05$, **- $p \leq 0.01$, and *** - $p \leq 0.001$ indicate significance levels.

Parameter (g m^{-2})		**T1**	**T2**	**T3**	**p - value**
AG vegetation	Biomass	207± 161	1753 ±2101	1095 ± 170	0.175
	C mass	66 ± 49	752 ± 866	554 ± 100	0.128
	N mass	1.5 ± 1.0	24 ± 30	11 ± 2.0	0.164
BG vegetation	Biomass	58 ± 78	1774 ± 385	2062 ± 411	***
	C mass	24 ± 34	753 ± 157	959 ± 183	***
	N mass	0.36 ± 0.5	20.0 ± 5.4	20.4 ± 6.3	***
Soil	C mass	40 ± 12	557 ± 115	384 ± 98	***
	N mass	22 ± 3.4	58 ± 10	59 ± 8.9	***

PeerJ Preprints | https://doi.org/10.7287/peerj.preprints.27703v1 | CC BY 4.0 Open Access | rec: 6 May 2019, publ: 6 May 2019

Table 3

Developed models to explain the observed fluxes using all environmental variables.

DW BG=dry weight of BG vegetation; Csoil=soil carbon; C BG=carbon content in BG vegetation; Nsoil=soil nitrogen; Tair=air temperature. Significance levels: value without asterisk $0.1 \leq p \leq 0.05$; *$p \leq 0.05$; **$p \leq 0.01$; *** $p \leq 0.001$. SE = Residual standard error.

Parameter	**Developed model**	**Multiple R-squared**	**p-value**	**SE**
NEE	NEE= -6.125023*-0.002048 DW BG -0.008529 Csoil+ 0.421186 Tair	0.4119	0.0001076	4.197
GEE	GEE=-2.975012*-0.001984*DW BG -0.013756**Csoil	0.5482	<0.0001	4.361
Reco	Reco=-2.9809733***-0.000953*C AG+0.0061722**DW BG-0.0132679**C BG+0.0722129*** Nsoil + 0.2600114***Tair	0.8057	<0.0001	0.9601

PeerJ Preprints | https://doi.org/10.7287/peerj.preprints.27703v1 | CC BY 4.0 Open Access | rec: 6 May 2019, publ: 6 May 2019